



# Compact ETD RK scheme for nonlinear dispersive wave equations

Muyassar Ahmat<sup>1</sup> · Jianxian Qiu<sup>2</sup>

Received: 16 May 2021 / Revised: 26 July 2021 / Accepted: 7 October 2021  
© SBMAC - Sociedade Brasileira de Matemática Aplicada e Computacional 2021

## Abstract

In this paper, a fourth-order scheme is presented for nonlinear dispersive wave equations. The scheme uses the fourth-order compact finite-difference method for discretization in space and the fourth-order exponential time-differencing Runge–Kutta (ETDRK) method for the temporal direction, respectively. The Cauchy integral formula takes effect on stabilizing the fourth-order ETD RK method, and deals with nondiagonal large sparse coefficient matrix which has complex eigenvalues tend to zero. It can be observed by numerical experiments that the numerical method is performed efficiently for the solitary wave profile of the Rosenau–KdV–RLW equation.

**Keywords** Nonlinear dispersive wave equation · Fourth-order compact finite-difference method · Fourth-order ETD Runge–Kutta method · Cauchy integral formula

**Mathematics Subject Classification** 65M60 · 35L65

## 1 Introduction

Many natural phenomena can be modeled by various nonlinear equations mathematically, and yet, it has been challenging to evaluate analytical and numerical solutions of these types

---

Communicated by Abdellah Hadjadj.

---

The research is partly supported by NSFC Grant 12071392.

---

✉ Jianxian Qiu  
jxqiu@xmu.edu.cn

Muyassar Ahmat  
muyassar@stu.xmu.edu.cn

<sup>1</sup> School of Mathematical Sciences, Xiamen University, Xiamen 361005, Fujian, People's Republic of China

<sup>2</sup> School of Mathematical Sciences and Fujian Provincial Key Laboratory of Mathematical Modeling and High-Performance Scientific Computing, Xiamen University, Xiamen 361005, Fujian, People's Republic of China

of nonlinear equations. The exact solutions of these nonlinear equations are always hard to be found, and even analytical solutions are barely available, because the nonlinear terms are included; therefore, numerical solutions are significantly essential. In this paper, we will focus on the numerical simulation of some nonlinear dispersive water wave models with power-law nonlinearity.

Water wave dynamics are usually explained by the KdV equation (Korteweg–de Vries equation) (Korteweg and De Vries 1895; Cui and Mao 2007; Bahadir 2005), the RLW equation (Regularized Long-Wave equation) Peregrine (1966, 1967), and the Rosenau equation (Rosenau 1986, 1988; Park 1990). The KdV equation describes small-amplitude long-wave behavior on the surface of the water in a channel. The RLW equation describes the undular bore behavior in water dynamics and simulates different situations of nonlinear dispersive waves for modeling a small-amplitude long wave in a channel. However, the wave–wave and wave–wall interaction cannot be explained by the KdV and RLW equations. This can be fulfilled by the Rosenau equation, because it is suitable for dense discrete system dynamics. For further more understanding of nonlinear wave behavior, viscous terms  $u_{xxt}$  and  $u_{xxx}$  need to be included in the Rosenau equation, which brings the achievement of Rosenau–RLW, Rosenau–KdV, and Rosenau–KdV–RLW equations. In this paper, we focus on the generalized initial-boundary value problem of the Rosenau–KdV–RLW equation with homogeneous boundary conditions given by

$$\begin{cases} u_t + \delta u_{xxt} + \nu u_{xxxxt} + \alpha u_x + \theta u_{xxx} + \varepsilon(u^p)_x = 0 & x \in (-\infty, +\infty), t \in (0, \infty) \\ u(x, 0) = u_0(x) & x \in (-\infty, +\infty) \\ u(\pm\infty, t) = u_x(\pm\infty, t) = u_{xx}(\pm\infty, t) = 0 & x \in (-\infty, +\infty), \end{cases} \quad (1.1)$$

where  $u(x, t)$  denotes the wave profile, and  $x$  and  $t$  are the spatial and temporal variables, respectively.  $\alpha > 0$ ,  $\varepsilon > 0$  are the parameters of linear and nonlinear advection term, and  $p \geq 2$  is the parameter of power-law nonlinearity.  $\theta$ ,  $\delta$ ,  $\nu$  are the parameters of KdV, RLW, and Rosenau terms, respectively. The equation (1.1) can be reduced to Rosenau–KdV equation with  $\delta = 0$  and Rosenau–RLW equation with  $\theta = 0$ .

In the field, a considerable amount of literature has been published to study the solitary wave behavior of these equations, for both theoretical and numerical analysis. A mass-preserving nonlinear method which combines a high-order compact scheme and a three-level average difference iterative algorithm was analyzed and tested for the Rosenau–RLW equation in Wongsaijai et al. (2019). This equation was also investigated by a conservative three-level linear-implicit finite difference method in Pan and Zhang (2012). An attempt has been made to propose a conservative finite-difference scheme for the Rosenau–RLW equation, which was unconditionally stable and the fourth order in space and the second order in time by Ghiloufi and Omrani (2017). Another fourth-order accurate three-level conservative linear finite-difference scheme was proposed by Hu and Wang (2013) for the Rosenau–RLW equation. A conservative unconditionally stable finite-difference scheme for 1D and 2D generalized Rosenau–KdV equation was proposed by Wang and Dai (2019) with fourth- and second-order accuracy in space and time, respectively. Wongsaijai and Pochinapan (2014) developed a three-level second-order accurate weighted average implicit finite-difference scheme to solve the Rosenau–KdV equation and Rosenau–KdV–RLW equation. A three-level linear conservative implicit finite-difference scheme was introduced by Wang and Dai (2017) for solving the Rosenau–KdV–RLW equation. This equation was simulated efficiently by a multi-symplectic scheme and an energy-preserving scheme in Cai et al. (2018) based on the multi-symplectic Hamiltonian formulation of the equation. The combination of a high efficient compact method for space and a trapezoidal method for time integration was

designed in Apolinar-Fernndez and Ramos (2018), and numerical analysis was given for the effects of the parameters with Gaussian initial conditions on wave behavior of these types of equations.

The high-order compact finite-difference scheme is one of several efficient numerical approaches (Lele 1992; Li 2008; Sari and Gürarlan 2009), and has been widely used for various types of partial differential equations(PDEs) in the last decade (Li and Visbal 2006; Gürarlan 2010; Zhao and Corless 2006; Wang and Zhang 2009). One can approximate derivatives of any order using much smaller stencils than same-order finite-difference methods using the relationship between the point and derivative values along a grid line and solving a linear tri-diagonal or penta-diagonal system of equations. However, the compact finite-difference scheme usually requires a very small time step to ensure numerical stability with explicit time solvers such as the explicit Runge–Kutta method. Therefore, methods with reliable stability prosperity should be adopted alongside.

The exponential time-differencing (ETD) method is an active and effective time solver with the advantages of solving linear part exactly and loosening the CFL restriction for stiff PDEs which contain linear and nonlinear terms and can be applied generally for this type of PDEs (Cox and Matthews 2002; Kassam and Trefethen 2005; Hochbruck and Ostermann 2005; Du and Zhu 2005; Qiu et al. 2019). However, the original high-order ETD Runge–Kutta (ETDRK) schemes (Cox and Matthews 2002) were proved to be unsuccessful because of disastrous cancellation error when the eigenvalue of the coefficient matrix in the linear part is equal to or close to zero, and also cannot be applied directly when the coefficient matrix in the linear term is nondiagonal. To overcome this difficulty, Kassam (Kassam and Trefethen 2005; Thacher 1974; Trefethen 2000) came up with one effective solution, which made use of the Cauchy integral formula to deal with removable singularity mathematically exact and numerically accurate. The stability analysis of the ETDRK scheme with the Cauchy integral formula was provided in Du and Zhu (2005). This point is very crucial in this paper, because the linear coefficient matrix of the above model obtained by the compact finite-difference method is always nondiagonal and has complex eigenvalues close to zero.

In Sect. 2, the fourth-order compact method in spatial discretization for (1.1) is described. In Sect. 3, the equal and more simple modified version of Cox’s fourth-order ETD scheme (Cox and Matthews 2002) and the Cauchy integral formula are given for the treatment in the time direction. Stability analysis for the linear version of (1.1) is given in Sect. 4. Extensive numerical tests are shown in Sect. 5 to illustrate the accuracy and efficiency of the present method for nonlinear wave motions.

## 2 Spatial discretization

We consider the Rosenau–KdV–RLW equation (1.1), and set computation domain as  $[x_l, x_r]$ .  $\Delta x$  is the cell size of the equally spaced grid in space. The uniform mesh is distributed as follows:

$$x \in [x_l, x_r], \quad \Delta x = \frac{x_r - x_l}{N - 1}, \quad x_j = x_l + (j - 1)\Delta x, \quad j = 1 : N.$$

The advection, convection, dispersion, and Rosenau terms are denoted as

$$a \equiv u_x, \quad c \equiv u_{xx}, \quad d \equiv u_{xxx}, \quad r \equiv u_{xxxx}. \tag{2.1}$$

The equation (1.1) can be rearranged as

$$(u + \delta c + vr)_t = (-\alpha a - \theta d) - \varepsilon pu^{p-1}a. \tag{2.2}$$



where

$$\begin{aligned}
 L &= (I + \delta \tilde{C}^{-1} J + \nu \tilde{C}^{-1} J \tilde{C}^{-1} J)^{-1} (-\alpha \tilde{A}^{-1} B - \theta \tilde{C}^{-1} J \tilde{A}^{-1} B), \\
 N_u(U) &= (I + \delta \tilde{C}^{-1} J + \nu \tilde{C}^{-1} J \tilde{C}^{-1} J)^{-1} (-\varepsilon p W \tilde{A}^{-1} B U).
 \end{aligned}
 \tag{2.8}$$

### 3 The fourth-order ETD RK method with Cauchy integral formula

The ordinary differential equation (2.7) has the formal solution

$$U^{n+1} = e^{\Delta t L} U^n + \int_0^{\Delta t} e^{(\Delta t - \tau)L} N_u(U(t_n + \tau)) d\tau,
 \tag{3.1}$$

where  $\Delta t$  is the temporal step size. This is the main path to propose an exponential time difference method in which the stiff linear part is computed analytically, whereas the nonlinear term is approximated numerically. Let  $Q = \frac{\Delta t L}{2}$ ,  $Z = \Delta t L$ , and then, the Cox and Matthews ETD RK4 (Cox and Matthews 2002) scheme is given as

$$\begin{aligned}
 U^{(1)} &= e^Q U^n + \frac{\Delta t}{2} \left( \frac{e^Q - I}{Q} \right) N_u(U^n, t_n), \\
 U^{(2)} &= e^Q U^n + \frac{\Delta t}{2} \left( \frac{e^Q - I}{Q} \right) N_u(U^{(1)}, t_n + \frac{\Delta t}{2}), \\
 U^{(3)} &= e^Q U^{(1)} + \frac{\Delta t}{2} \left( \frac{e^Q - I}{Q} \right) \left( 2N_u(U^{(2)}, t_n + \frac{\Delta t}{2}) - N_u(U^n, t_n) \right), \\
 U^{n+1} &= e^Z U^n + \Delta t Z^{-3} \left[ -4I - Z + e^Z (4I - 3Z + Z^2) \right] N_u(U^n, t_n) \\
 &\quad + \Delta t Z^{-3} \left[ 4I + 2Z + 2e^Z (-2I + Z) \right] \left( N_u(U^{(1)}, t_n + \frac{\Delta t}{2}) + N_u(U^{(2)}, t_n + \frac{\Delta t}{2}) \right) \\
 &\quad + \Delta t Z^{-3} \left[ -4I - 3Z - Z^2 + e^Z (4I - Z) \right] N_u(U^{(3)}, t_n + \Delta t),
 \end{aligned}
 \tag{3.2}$$

where  $I$  is  $N \times N$  identity matrix. To write (3.2) in modified form, first, we refer the matrix exponential  $\psi_k(v) = \sum_{j=0}^{\infty} \frac{v^j}{(j+k)!}$  functions

$$\psi_0(v) = e^v, \quad \psi_1(v) = \frac{e^v - 1}{v}, \quad \psi_2(v) = \frac{e^v - 1 - v}{v^2}, \quad \psi_3(v) = \frac{e^v - 1 - v - \frac{1}{2}v^2}{v^3}, \dots
 \tag{3.3}$$

The  $\psi_k(v)$  satisfies the recurrence relation

$$\psi_k(v) = v\psi_{k+1}(v) + \frac{1}{k!}
 \tag{3.4}$$

as

$$\psi_2(v) = v\psi_3(v) + \frac{1}{2}, \quad \psi_1(v) = v\psi_2(v) + 1 = v^2\psi_3(v) + \frac{1}{2}v + 1.
 \tag{3.5}$$

Now, we rewrite the coefficients in the update formula (3.2) of ETD RK4 as the linear combination of the above exponential  $\psi$  functions

$$\begin{aligned}
 M_0(Q) &= e^Q = \psi_0(Q), \quad M_0(Z) = e^Z = \psi_0(Z), \quad M_1(Q) = \frac{e^Q - I}{Q} = \psi_1(Q), \\
 M_2(Z) &= Z^{-3} \left[ -4I - Z + e^Z (4I - 3Z + Z^2) \right]
 \end{aligned}$$

$$\begin{aligned}
 &= 4\psi_3(Z) - 3Z\psi_3(Z) + Z^2\psi_3(Z) + \frac{1}{2}Z - \frac{1}{2}I, \\
 M_3(Z) &= Z^{-3} \left[ 4I + 2Z + 2e^Z(-2I + Z) \right] = -4\psi_3(Z) + 2Z\psi_3(Z) + I, \\
 M_4(Z) &= Z^{-3} \left[ -4I - 3Z - Z^2 + e^Z(4I - Z) \right] = 4\psi_3(Z) - Z\psi_3(Z) - \frac{1}{2}I.
 \end{aligned}
 \tag{3.6}$$

If the ETDRK4 scheme is evaluated with these coefficients directly, the numerical scheme will be unstable because of the cancellation error on the calculation of  $\psi_0(Q)$ ,  $\psi_1(Q)$ ,  $\psi_0(Z)$ ,  $\psi_3(Z)$ . To reduce the numerical instability caused by cancellation error in high-order ETD and ETD Runge–Kutta schemes, the modified ETD scheme was proposed in Kassam and Trefethen (2005) using the Cauchy integral formula to evaluate the linear exponentials which are used in the nonlinearities in (3.2) for ETDRK4 and also achieved the effort of generalizing the ETD schemes to nondiagonal problems. The Cauchy integral theory was introduced in detail in Thacher (1974); Trefethen (2000), while the stability analysis and truncation error analysis on modified ETD scheme with Cauchy integral formula were given in Du and Zhu (2005).

Here, we choice to use contour  $C_o$  in the complex plane that encloses all the eigenvalues of  $Z$  and well separated from 0 to evaluate  $\psi_0(Q)$ ,  $\psi_1(Q)$  and  $\psi_0(Z)$ ,  $\psi_3(Z)$

$$f(Z) = \frac{1}{2\pi i} \int_{C_o} f(t)(tI - Z)^{-1} dt.
 \tag{3.7}$$

The contour  $C_o$  consist of several equally spaced points, usually 32 or 64 points are sufficient; see Kassam and Trefethen (2005); Du and Zhu (2005). The specific Matlab code for using the Cauchy integral in practice can be found in Kassam and Trefethen (2005). The spectrum of  $L$  increases along with  $\Delta t$  decreases, so the spectrum of  $Z = L\Delta t$  still can be bounded in certain contour as long as we choose the radius of the contour carefully. In Du and Zhu (2005), some analyses have been proceeded on this topic. It is pointed out that if the radius is no more than a quarter of the number of quadrature points, the stability region will not be affected significantly.

For this nonlinear dispersive problem, the eigenvalues of  $Z$  are always close to the imaginary axis. Here, we take the simplest approach in which the contour  $C_o$  is a circle of radius  $r_o = \text{ceil}(\max(|\text{eig}(Z)|))$  centered at 0, so that we can always make sure that all eigenvalues of  $Z$  are in this contour in any case of  $\Delta t$ . The quadrature angles of the contour are taken as  $\theta = [\frac{\pi}{32}, \frac{3\pi}{32}, \dots, \frac{63\pi}{32}]$  sampled at 32 equally spaced points  $z = r_o\theta$ .

The modification of these coefficients in the above complex circle was given in Kassam and Trefethen (2005); Thacher (1974) as

$$\begin{aligned}
 \psi_0(Q) &= \frac{1}{2\pi i} \int_{C_o} \psi_0(z)(zI - Q)^{-1} dz = \frac{1}{2\pi} \int_0^{2\pi} e^z z(zI - Q)^{-1} d\theta, \\
 \psi_1(Q) &= \frac{1}{2\pi i} \int_{C_o} \psi_1(z)(zI - Q)^{-1} dz = \frac{1}{2\pi} \int_0^{2\pi} (e^z - 1)(zI - Q)^{-1} d\theta, \\
 \psi_0(Z) &= \frac{1}{2\pi i} \int_{C_o} \psi_0(z)(zI - Z)^{-1} dz = \frac{1}{2\pi} \int_0^{2\pi} e^z z(zI - Z)^{-1} d\theta,
 \end{aligned}$$

$$\psi_3(Z) = \frac{1}{2\pi i} \int_{C_0} \psi_3(z)(zI - Z)^{-1} dz = \frac{1}{2\pi} \int_0^{2\pi} \frac{e^z - 1 - z - \frac{1}{2}z^2}{z^2} (zI - Z)^{-1} d\theta. \tag{3.8}$$

We have

$$\begin{aligned} q_1(z) &= e^z z(zI - Q)^{-1}, \quad q_2(z) = (e^z - 1)(zI - Q)^{-1}, \\ q_3(z) &= e^z z(zI - Z)^{-1}, \quad q_4(z) = \frac{e^z - 1 - z - \frac{1}{2}z^2}{z^2} (zI - z)^{-1}. \end{aligned} \tag{3.9}$$

We obtain the modified version of these coefficients in complex plane by the means of exponentially fast converging trapezoid rule

$$\begin{aligned} \tilde{\psi}_0(Q) &= \frac{1}{32} \sum_{s=1}^{32} q_1(z_s), \quad \tilde{\psi}_1(Q) = \frac{1}{32} \sum_{s=1}^{32} q_2(z_s), \\ \tilde{\psi}_0(Z) &= \frac{1}{32} \sum_{s=1}^{32} q_3(z_s), \quad \tilde{\psi}_3(Z) = \frac{1}{32} \sum_{s=1}^{32} q_4(z_s). \end{aligned} \tag{3.10}$$

Finally, we make use of above  $\tilde{\psi}_0(Q)$ ,  $\tilde{\psi}_1(Q)$ ,  $\tilde{\psi}_0(Z)$ ,  $\tilde{\psi}_3(Z)$  to evaluate the coefficients  $M_0(Q)$ ,  $M_0(Z)$ ,  $M_1(Q)$ ,  $M_2(Z)$ ,  $M_3(Z)$ ,  $M_4(Z)$

$$\begin{aligned} \tilde{M}_0(Q) &= \tilde{\psi}_0(Q), \quad \tilde{M}_1(Q) = \tilde{\psi}_1(Q), \quad \tilde{M}_0(Z) = \tilde{\psi}_0(Z), \\ \tilde{M}_2(Z) &= 4\tilde{\psi}_3(Z) - 3Z\tilde{\psi}_3(Z) + Z^2\tilde{\psi}_3(Z) + \frac{1}{2}Z - \frac{1}{2}I, \\ \tilde{M}_3(Z) &= -4\tilde{\psi}_3(Z) + 2Z\tilde{\psi}_3(Z) + I, \\ \tilde{M}_4(Z) &= 4\tilde{\psi}_3(Z) - Z\tilde{\psi}_3(Z) - \frac{1}{2}I. \end{aligned} \tag{3.11}$$

In this way, we can efficiently avoid extra computation and cancellation error caused by high-order matrix inversion on coefficients, since most of them are expressed by the matrix product of  $\psi_3(Z)$  and power function of  $Z$ . We have the final fourth-order ETD Runge–Kutta scheme takes the form as

$$\begin{aligned} U^{(1)} &= \tilde{M}_0(Q)U^n + \frac{\Delta t}{2} \tilde{M}_1(Q)N_u(U^n, t_n), \\ U^{(2)} &= \tilde{M}_0(Q)U^n + \frac{\Delta t}{2} \tilde{M}_1(Q)N_u(U^{(1)}, t_n + \frac{\Delta t}{2}), \\ U^{(3)} &= \tilde{M}_0(Q)U^{(1)} + \frac{\Delta t}{2} \tilde{M}_1(Q) \left( 2N_u(U^{(2)}, t_n + \frac{\Delta t}{2}) - N_u(U^n, t_n) \right), \\ U^{n+1} &= \tilde{M}_0(Z)U^n + \Delta t \tilde{M}_2(Z)N_u(U^n, t_n) + \Delta t \tilde{M}_3(Z) \left( N_u(U^{(1)}, t_n + \frac{\Delta t}{2}) \right. \\ &\quad \left. + N_u(U^{(2)}, t_n + \frac{\Delta t}{2}) \right) + \Delta t \tilde{M}_4(Z)N_u(U^{(3)}, t_n + \Delta t). \end{aligned} \tag{3.12}$$

### 4 Linear stability of the fourth-order ETD Runge–Kutta method with Cauchy integral

Here, we give stability property of (3.12) for the linear scalar version of (1.1) with  $p = 1$ . Use of  $u_j = \bar{u}e^{ikj\Delta x}$ ,  $a_j = \bar{a}e^{ikj\Delta x}$ ,  $c_j = \bar{c}e^{ikj\Delta x}$  at  $(x_j, t)$ , the Fourier relationship between varying spacial derivatives in (2.3) and (2.4) are

$$\begin{aligned} \bar{a} &= \bar{u} \frac{i \sinh(k \Delta x)}{\Delta x \left(\frac{1}{3} \cosh(k \Delta x) + \frac{2}{3}\right)}, \quad \bar{c} = \bar{u} \frac{2 \cosh(k \Delta x) - 2}{\Delta x^2 \left(\frac{1}{6} \cosh(k \Delta x) + \frac{5}{6}\right)}, \\ \bar{d} &= \bar{a} \frac{2 \cosh(k \Delta x) - 2}{\Delta x^2 \left(\frac{1}{6} \cosh(k \Delta x) + \frac{5}{6}\right)}, \quad \bar{r} = \bar{c} \frac{2 \cosh(k \Delta x) - 2}{\Delta x^2 \left(\frac{1}{6} \cosh(k \Delta x) + \frac{5}{6}\right)}. \end{aligned} \tag{4.1}$$

The scalar linear version of (2.7) yields

$$\bar{u}_t = l\bar{u} + \lambda\bar{u}, \tag{4.2}$$

where

$$\begin{aligned} l &= \frac{-\alpha \frac{i \sinh(k \Delta x)}{\Delta x \left(\frac{1}{3} \cosh(k \Delta x) + \frac{2}{3}\right)} - \theta \frac{i \sinh(k \Delta x)}{\Delta x \left(\frac{1}{3} \cosh(k \Delta x) + \frac{2}{3}\right)} \frac{2 \cosh(k \Delta x) - 2}{\Delta x^2 \left(\frac{1}{6} \cosh(k \Delta x) + \frac{5}{6}\right)}}{1 + \delta \frac{2 \cosh(k \Delta x) - 2}{\Delta x^2 \left(\frac{1}{6} \cosh(k \Delta x) + \frac{5}{6}\right)} + \nu \left(\frac{2 \cosh(k \Delta x) - 2}{\Delta x^2 \left(\frac{1}{6} \cosh(k \Delta x) + \frac{5}{6}\right)}\right)^2}, \\ \lambda &= \frac{-\varepsilon \frac{i \sinh(k \Delta x)}{\Delta x \left(\frac{1}{3} \cosh(k \Delta x) + \frac{2}{3}\right)}}{1 + \delta \frac{2 \cosh(k \Delta x) - 2}{\Delta x^2 \left(\frac{1}{6} \cosh(k \Delta x) + \frac{5}{6}\right)} + \nu \left(\frac{2 \cosh(k \Delta x) - 2}{\Delta x^2 \left(\frac{1}{6} \cosh(k \Delta x) + \frac{5}{6}\right)}\right)^2}. \end{aligned}$$

Recall the approximation of the two-point quadrature amount in scalar case

$$\frac{e^{\frac{l\Delta t}{2}} - 1}{l} \sim \frac{1}{2} \left( \frac{e^{\frac{(l+r_0i)\Delta t}{2}} - 1}{l + r_0i} + \frac{e^{\frac{(l-r_0i)\Delta t}{2}} - 1}{l - r_0i} \right), \tag{4.3}$$

where  $r_0i$  and  $-r_0i$  are so chosen as the quadrature points for the approximation of the contour integral in contour with radius  $r_0$  and centered at 0 in this paper. Simplify the right-hand side of (4.3) and let

$$\frac{e^{\frac{l\Delta t}{2}} - 1}{l} \sim \frac{le^{\frac{l\Delta t}{2}} \cos\left(\frac{r_0\Delta t}{2}\right) + r_0e^{\frac{l\Delta t}{2}} \sin\left(\frac{r_0\Delta t}{2}\right) - l}{l^2 + r_0^2} = \phi. \tag{4.4}$$

From (3.2), we can write  $\bar{u}^{(1)}$ ,  $\bar{u}^{(2)}$ ,  $\bar{u}^{(3)}$ , and the corresponding amplification factors as

$$\begin{aligned} \bar{u}^{(1)} &= \left(e^{\frac{l\Delta t}{2}} + \phi\lambda\right)\bar{u}, \quad g^{(1)} = e^{\frac{l\Delta t}{2}} + \phi\lambda, \\ \bar{u}^{(2)} &= \left(e^{\frac{l\Delta t}{2}} + \phi\lambda g^{(1)}\right)\bar{u}, \quad g^{(2)} = e^{\frac{l\Delta t}{2}} + \phi\lambda g^{(1)}, \\ \bar{u}^{(3)} &= \left(e^{\frac{l\Delta t}{2}} g^{(1)} + \phi\lambda(2g^{(2)} - 1)\right)\bar{u}, \quad g^{(3)} = e^{\frac{l\Delta t}{2}} g^{(1)} + \phi\lambda(2g^{(2)} - 1). \end{aligned} \tag{4.5}$$

Using these, we finally can derive the corresponding amplification factor

$$G(l, \lambda) = e^{l\Delta t} + \varphi_1\lambda + \varphi_2\lambda(g^{(1)} + g^{(2)}) + \varphi_3\lambda g^{(3)}; \tag{4.6}$$

here,  $\varphi_1 = \frac{-4-l\Delta t + (\phi l + 1)^2(4-3l\Delta t + \Delta t^2 l^2)}{\Delta t^2 l^3}$ ,  $\varphi_2 = \frac{4+2l\Delta t + 2(\phi l + 1)^2(-2+l\Delta t)}{\Delta t^2 l^3}$ ,

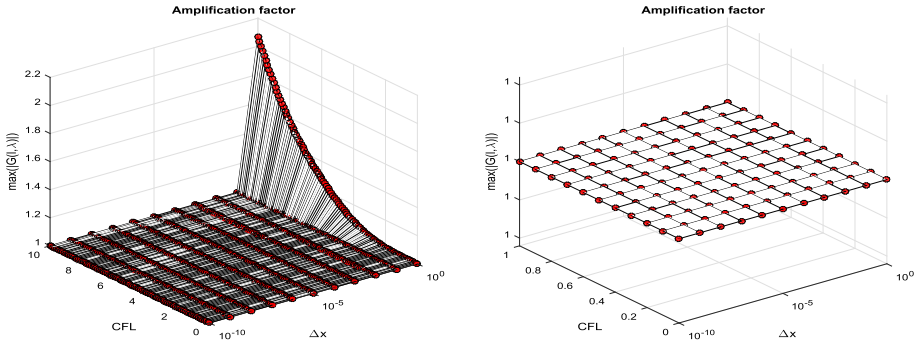


**Fig. 1** Amplification factor for varies CFL and  $\Delta x$  for the linear version of (1.1) with parameters  $\delta = -1, \nu = 1, \theta = 1, \alpha = 0, \varepsilon = 1, p = 1$ (left) and the partial graph of amplification factor for  $CFL = [0, 1], \Delta x = [10^{(-10)}, 1]$ (right)

$$\varphi_3 = \frac{-4 - 3l\Delta t - \Delta t^2 l^2 + (\phi l + 1)^2 (4 - l\Delta t)}{\Delta t^2 l^3}$$

In Du and Zhu (2005), significant analysis is given in the case of  $l$  is negative real, while  $\lambda$  is complex, and both  $l, \lambda$  are real. Notice that in our case,  $l$  and  $\lambda$  are both complex, which still remains as an open problem. Unfortunately, we do not know any expression for  $|G(l, \lambda)| \leq 1$ .

To demonstrate the stability prosperity of the scheme, we compute the amplification factor  $|G(l, \lambda)|$  for various  $CFL = \frac{\Delta t}{\Delta x}$  and  $\Delta x$  for the linear version of (1.1) with parameters  $\delta = -1, \nu = 1, \theta = 1, \alpha = 0, \varepsilon = 1, p = 1$ . Notice that in computing  $\phi, g^{(1)}, g^{(2)}, g^{(3)}, \varphi_1, \varphi_2, \varphi_3$  suffer from numerical instability for  $l$  and  $\Delta t$  close to zero. Because of that, we will use their five-term Taylor expansions in computational process. In Fig. 1(left), we take  $CFL = [0, 10], \Delta x = [10^{(-10)}, 1]$  and  $\Delta t = CFL \cdot \Delta x$ .

It can be observed that  $|G(l, \lambda)|$  gets bigger than 1 with small increase along with the increase in  $CFL$  and  $\Delta x$ . Figure 1(right) is the partial graph for  $CFL = [0, 1], \Delta x = [10^{(-10)}, 1]$ . In this paper, we take  $CFL = 1, \Delta x = \Delta t \leq 0.4$  for all numerical simulation to ensure the numerical stability of the scheme for equation (1.1).

### 5 Numerical results

In this section, The algorithm (3.12) is applied through the Rosenau–RLW equation, Rosenau–KdV equation, and Rosenau–KdV–RLW equation to confirm the performance of the present method. The advantages of the ETD method allow us to take a large time step, so that  $\Delta t = CFL \cdot \Delta x$  with  $CFL = 1$  is sufficiently enough for fourth-order convergence rate both in space and time in terms of  $L_2$  and  $L_\infty$  for each test cases. The corresponding contour and eigenvalues of each test cases are also plotted.

**Example 1** Considering Rosenau–RLW equation (1.1) with parameters  $\delta = -1, \nu = 1, \alpha = 1, \varepsilon = \frac{1}{2}, p = 2$

$$u_t - u_{xxt} + u_{xxxxt} + u_x + \frac{1}{2}(u^2)_x = 0, \quad x \in [-50, 150], t \in [0, T],$$

with the initial condition  $u(x, 0) = \frac{15}{19} \operatorname{sech}^4\left(\frac{\sqrt{13}}{26}x\right)$  and the analytical solitary wave solution

$$u(x, t) = \frac{15}{19} \operatorname{sech}^4\left(\frac{\sqrt{13}}{26}(x - \frac{169}{133}t)\right).$$

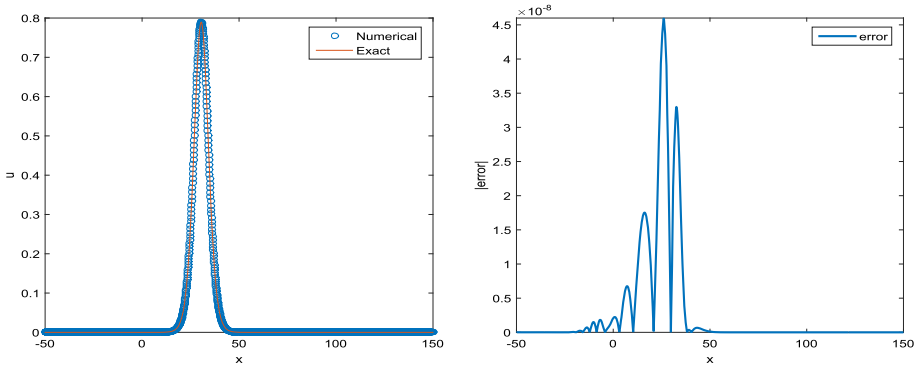


**Fig. 2** Numerical solution of Rosenau–RLW equation with  $CFL = 1$ ,  $\Delta x = \Delta t = 0.1$  at  $T = 24$  in interval  $x \in [-50, 150]$  (left) and error (right) for Example 1

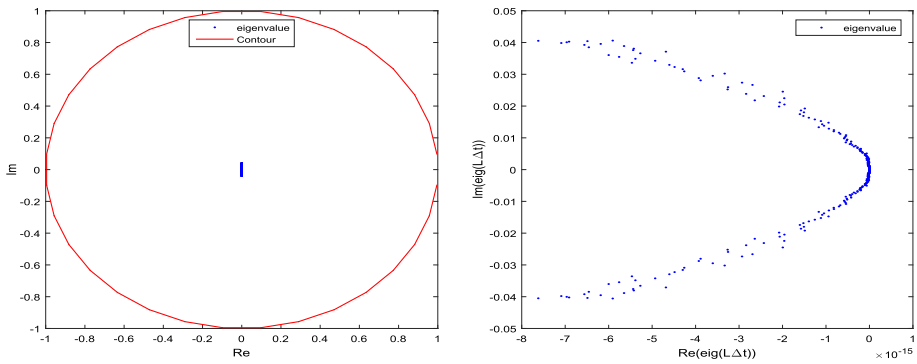


**Fig. 3** The eigenvalues and the corresponding contour with  $CFL = 1$ ,  $\Delta x = \Delta t = 0.1$  for Example 1

Numerical solutions on various mesh sizes are calculated and compared with the exact solution of the Rosenau–RLW equation. We model a solitary wave approximately and present the errors and rates of convergence in terms of  $L_2$  and  $L_\infty$  of the simulation at  $T = 24$  for  $\Delta t = CFL \cdot \Delta x$  with  $CFL = 1$  over interval  $x \in [-50, 150]$ . Numerical results are compared with previously published studies assessed in the introduction on Rosenau–RLW equation under same mesh in Table 1. We can see that experimental results agree with the theoretical fourth-order convergence rate in the case  $\Delta x = \Delta t$ .

Figure 2(left) shows that the solitary wave curve matches excellently with exact solution when  $\Delta x = \Delta t = 0.1$  at  $T = 24$  over interval  $x \in [-50, 150]$ . From Fig. 2(right), it can be seen that error mostly generates at two sides of the solitary wave peak. The eigenvalues and corresponding Contour are also plotted in this case in Fig. 3. Several right-propagating waves with almost identical amplitude are generated in Fig. 4 at different times  $T = 0, 10, 20$ . Solitary wave moves far away from its generation location through time with unchanged shape.

**Example 2** Considering Rosenau–KdV equation (1.1) with parameters  $\delta = 0, \nu = 1, \alpha = 1, \theta = 1, \varepsilon = \frac{1}{2}, p = 2$

$$u_t + u_{xxxxt} + u_{xxx} + u_x + \left(\frac{1}{2}u^2\right)_x = 0, \quad x \in [-70, 100], t \in [0, T].$$

**Table 1** Errors and rates of convergence of numerical solutions at  $T = 24$  with  $CFL = 1$ ,  $\Delta x = \Delta t$  in interval  $x \in [-50, 150]$  for Example 1

$\Delta x$	Ref. Pan and Zhang (2012)		Ref. Wongsajjai and Poochinapan (2014) $(-\frac{1}{3})$		Ref. Wongsajjai et al. (2019)		Present	
	$L_2$	Order	$L_2$	Order	$L_2$	Order	$L_2$	Order
0.4	6.5879e-02		4.8875e-03		4.7303e-05		2.1477e-06	
0.2	1.6846e-02	1.9673	1.2131e-03	2.0104	2.9407e-06	4.0076	1.3361e-07	4.0067
0.1	4.2394e-03	1.9905	3.0297e-04	2.0014	1.8377e-07	4.0018	8.3502e-09	4.0000
0.05	1.0623e-03	1.9967	7.5769e-05	1.9995	1.2753e-08	3.8490	5.2493e-10	3.9916
$\Delta x$	$L_\infty$	Order	$L_\infty$	Order	$L_\infty$	Order	$L_\infty$	Order
0.4	2.4843e-02		1.8240e-03		1.8720e-05		1.1827e-05	
0.2	6.3640e-03	1.9673	4.6918e-04	1.9589	1.1652e-06	4.0059	7.3494e-07	4.0083
0.1	1.1298e-04	1.9905	1.1827e-04	1.9881	7.2777e-08	4.0025	4.5947e-08	3.9996
0.05	2.8310e-05	1.9967	2.9691e-05	1.9940	5.2026e-09	3.8062	2.9034e-09	3.9841

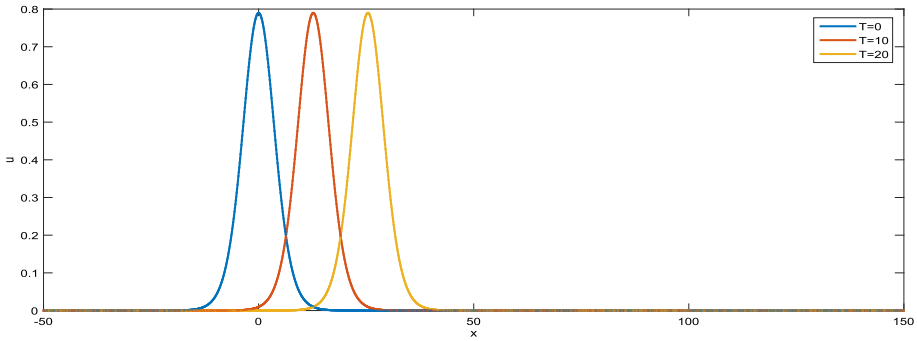


**Fig. 4** Wave graph of Rosenau–RLW equation with  $CFL = 1$ ,  $\Delta x = \Delta t = 0.1$  at  $T = 0, 10, 20$  in interval  $x \in [-50, 150]$  for Example 1

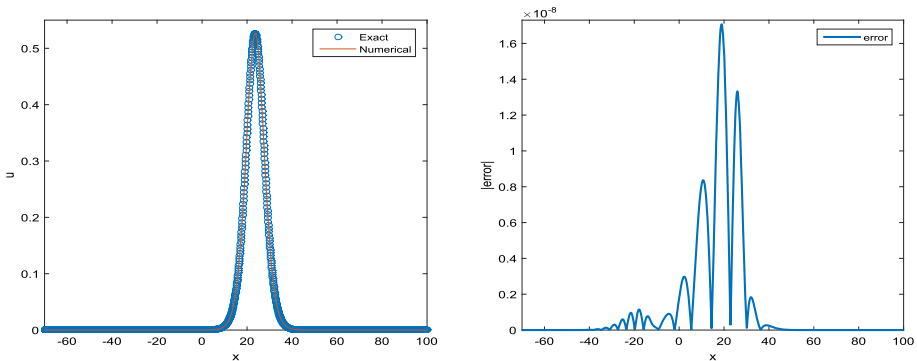


**Fig. 5** Numerical solution of Rosenau–KdV equation with  $CFL = 1$ ,  $\Delta x = \Delta t = 0.1$  at  $T = 20$  in interval  $x \in [-70, 100]$  for Example 2

Rosenau–KdV equation has the analytical solitary wave solution  $u(x, t) = M \operatorname{sech}^{\frac{4}{p-1}} [W(x - Vt)]$  as in Razborova et al. (2013) with wave width

$$W = \frac{p-1}{p+1} \left[ \frac{-\alpha v(p^2+2p+5) + \sqrt{\alpha^2 v^2(p^2+2p+5)^2 + 16\theta^2 v(p+1)^2}}{32\theta v} \right]^{\frac{1}{2}}, \text{ wave amplitude}$$

$$M = \left[ \frac{[-\alpha v(p^2+2p+5) + \sqrt{\alpha^2 v^2(p^2+2p+5)^2 + 16\theta^2 v(p+1)^2}](p+3)(3p+1)}{16v\epsilon(p+1)(p^2+2p+5)} \right]^{\frac{1}{p-1}}, \text{ and wave velocity}$$

$$V = \frac{\theta(p-1)^2}{4vW^2(p^2+2p+5)}. \text{ Here, we take the initial condition to be } u(x, 0) = M \operatorname{sech}^{\frac{4}{p-1}}(Wx).$$

We simulate this solitary wave problem under various meshes. The calculated errors, and rates of convergence in terms of  $L_2$  and  $L_\infty$  at  $T = 20$  for  $\Delta t = CFL \cdot \Delta x$  over interval  $x \in [-70, 100]$  are listed in Table 2. It can be observed that the present scheme has the smallest error with fourth-order convergence than the other three numerical schemes under the same mesh.

The solution profile and distribution of absolute error are shown in the right and left of Fig. 5 for  $\Delta x = \Delta t = 0.1$  at time  $T = 20$ . It seems that the maximum error occurs near the peak amplitude of the solitary wave. The eigenvalues and contour for this problem also can be seen in Fig. 6. The initial solitary wave at  $T = 0$  and numerical solutions at  $T = 10, 20$  with  $\Delta x = \Delta t = 0.1$  are given in Fig. 7.

**Table 2** Errors and rates of convergence of numerical solutions at  $T = 20$  with  $CFL = 1$ ,  $\Delta x = \Delta t$  in  $x \in [-70, 100]$  for Example 2

$\Delta x$	Ref. Wang and Dai (2017)		Ref. Wongsajjai and Poochinapan (2014)(1/3)		Ref. Wongsajjai and Poochinapan (2014)(-1/3)		Present	
	$L_2$	Order	$L_2$	Order	$L_2$	Order	$L_2$	Order
0.4	3.5253e-03		7.2210e-03		1.0810e-02		9.0518e-07	
0.2	9.0021e-04	1.9694	1.7779e-03	2.0221	2.6375e-03	2.0351	5.6380e-08	4.0049
0.1	1.1334e-04	1.9895	4.4396e-04	2.0017	6.5783e-04	2.0034	3.5245e-09	3.9997
0.05	1.4196e-05	1.9971	1.1098e-04	2.0000	1.6441e-04	2.0003	2.2550e-10	3.9662
$\Delta x$	$L_\infty$	Order	$L_\infty$	Order	$L_\infty$	Order	$L_\infty$	Order
0.4	3.4062e-03		1.9823e-03		4.1307e-03		4.3873e-06	
0.2	7.8920e-04	2.1097	4.9510e-04	2.0014	1.0191e-03	2.0190	2.7300e-07	4.0064
0.1	1.8771e-04	2.0718	1.2372e-04	2.0005	2.5411e-04	2.0038	1.7073e-08	3.9991
0.05	4.6987e-05	1.9981	3.0934e-05	1.9998	6.3501e-05	2.0006	1.0890e-09	3.9706

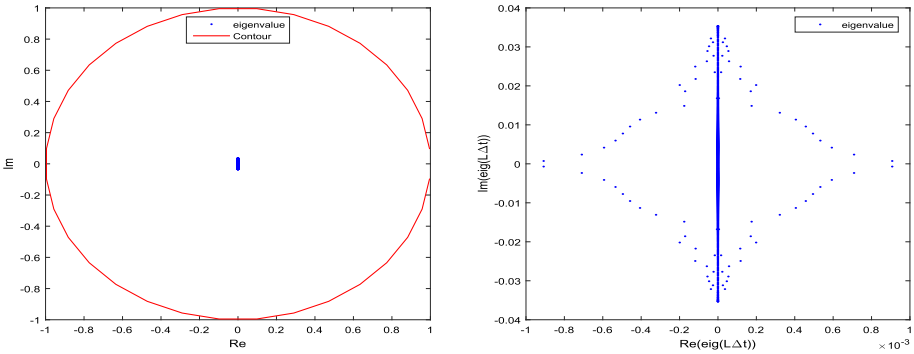


**Fig. 6** The eigenvalues and the corresponding Contour with  $CFL = 1, \Delta x = \Delta t = 0.1$  for Example 2

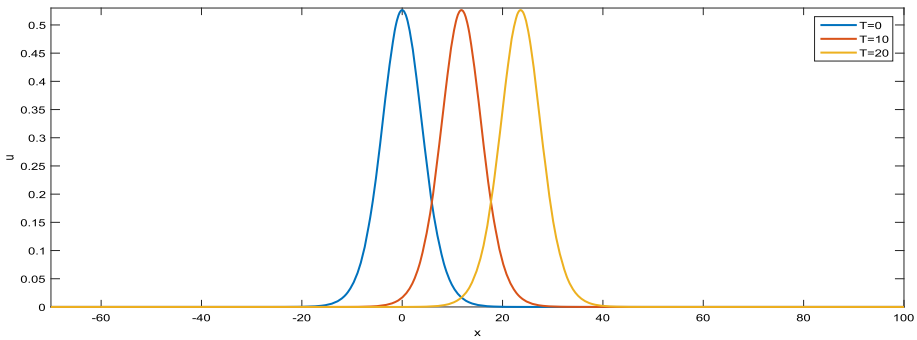


**Fig. 7** Wave graph of Rosenau-KdV equation with  $CFL = 1, \Delta x = \Delta t = 0.1$  at  $T = 0, 10, 20$  in interval  $x \in [-70, 100]$  for Example 2

**Example 3** Considering Rosenau-KdV-RLW equation (1.1) with parameters  $\delta = -1, \nu = 1, \alpha = 1, \theta = 1, \varepsilon = \frac{1}{2}, p = 2$

$$u_t - u_{xxt} + u_{xxxxt} + u_x + u_{xxx} + \frac{1}{2}(u^2)_x = 0, \quad x \in [-40, 60], t \in [0, T].$$

Rosenau-KdV-RLW equation has solitary wave solution  $u(x, t) = M \operatorname{sech}^{\frac{4}{p-1}} [W(x - Vt)]$  with  $S = \sqrt{\alpha^2 \nu^2 (p^2 + 2p + 5)^2 + 16(p + 1)^2 \theta \nu (\theta - \alpha \delta)}$ , wave width  $W = \frac{p-1}{p+1} \sqrt{\frac{S - (p^2 + 2p + 5)\alpha \nu}{32\theta \nu}}$ , wave speed  $V = \frac{\theta(p-1)^2}{(p-1)^2 \delta + 4\nu W^2 (p^2 + 2p + 5)}$ , and amplitude  $M = \left[ \frac{8(p+1)(p+3)(3p+1)\theta \nu W^4}{\varepsilon(p-1)^2 ((p-1)^2 \delta + 4(p^2 + 2p + 5)\nu W^2)} \right]^{\frac{1}{p-1}}$ . Here, we choose the initial condition to be  $u(x, 0) = M \operatorname{sech}^{\frac{4}{p-1}} (Wx)$ .

We report the calculated errors, and rates of convergence in terms of  $L_2$  and  $L_\infty$  at  $T = 10$  for  $\Delta t = CFL \cdot \Delta x$  with  $CFL = 1$  over interval  $x \in [-40, 60]$  in Table 3. We make comparison on the computation errors and convergence rates among three different numerical schemes to illustrate the superiority of present scheme (3.12) under the same mesh. Figure 8(left) presents numerical solitary wave profile for  $\Delta x = \Delta t = 0.1$  at time  $T = 10$ , which is close to analytical values. Figure 8(right) presents the corresponding distribution of absolute errors at time  $T = 10$ . The eigenvalues and contour for this problem are plotted in Fig. 9. Furthermore, Fig. 10 indicates that the right-propagating solitary wave profile travels

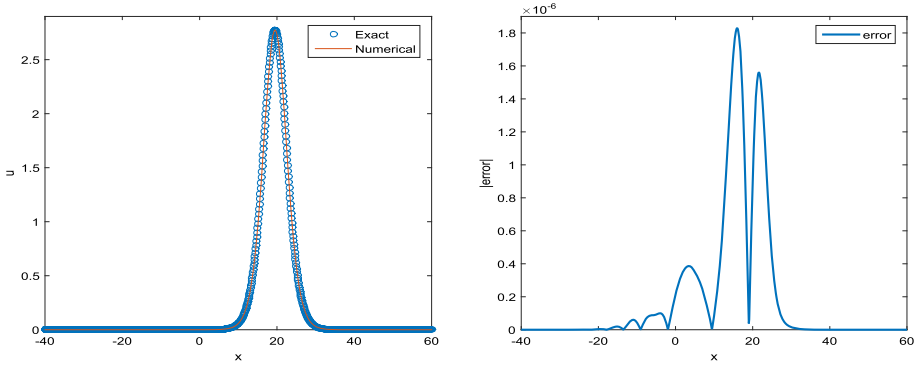


**Fig. 8** Numerical solution of Rosenau–KDV–RLW equation with  $CFL = 1$ ,  $\Delta t = \Delta x = 0.1$  at  $T = 10$  in interval  $x \in [-40, 60]$  (left) and error (right) for Example 3

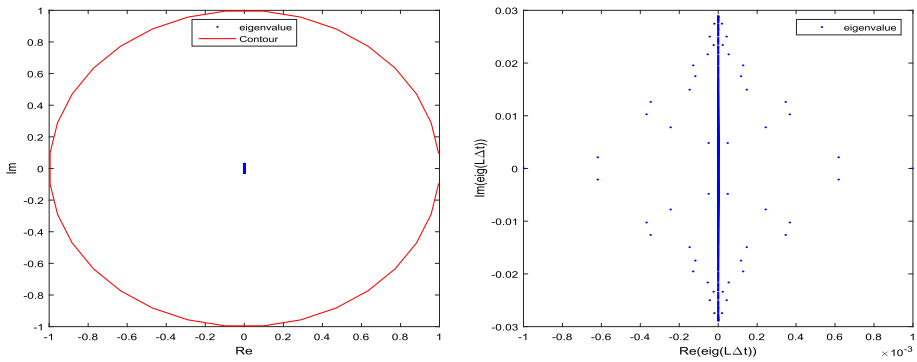


**Fig. 9** The eigenvalues and the corresponding Contour with  $CFL = 1$ ,  $\Delta x = \Delta t = 0.1$  for Example 3

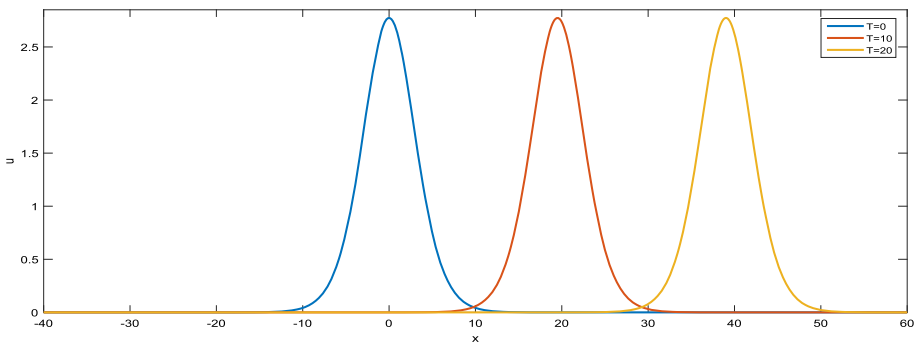


**Fig. 10** Wave graph of Rosenau–KDV–RLW equation with  $CFL = 1$ ,  $\Delta t = \Delta x = 0.1$  at  $T = 0, 10, 20$  in interval  $x \in [-40, 60]$  for Example 3

with unchanged shape and amplitude of the same height through times  $T = 0, 10, 20$  under  $\Delta x = \Delta t = 0.1$ .

**Table 3** Errors and rates of convergence of numerical solutions at  $T = 10$  with  $CFL = 1$ ,  $\Delta t = \Delta x$  in interval  $x \in [-40, 60]$  for Example 3

$h$	Ref. Wang and Dai (2017)		Ref. Wongsajjai and Poochinapan (2014)(1/3)		Ref. Wongsajjai and Poochinapan (2014)(-1/3)		Present	
	$L_2$	Order	$L_2$	Order	$L_2$	Order	$L_2$	Order
0.4	7.4574e-03		3.0408e-03		1.3079e-03		1.2671e-04	
0.2	1.9121e-03	1.9635	7.6263e-04	1.9954	3.1337e-04	2.0613	7.5823e-06	4.0628
0.1	4.8500e-04	1.9791	1.9101e-04	1.9973	7.7996e-05	2.0064	4.5951e-07	4.0445
0.05	1.2151e-04	1.9969	4.7789e-05	1.9989	1.9500e-05	1.9999	2.8829e-08	3.9945
$h$	$L_\infty$	Order	$L_\infty$	Order	$L_\infty$	Order	$L_\infty$	Order
0.4	3.9574e-03		2.7408e-03		1.1016e-03		4.6787e-04	
0.2	1.0062e-03	1.9756	6.8763e-04	1.9949	2.6194e-04	2.0723	2.9429e-05	3.9908
0.1	2.5353e-04	1.9887	1.7237e-04	1.9961	6.5114e-05	2.0082	1.8288e-06	4.0083
0.05	6.3492e-05	1.9975	4.3140e-05	1.9984	1.6295e-05	1.9985	1.1597e-07	3.9791

## 6 Concluding remark

The fourth-order compact finite-difference method for spatial discretization and fourth-order ETDRK method with Cauchy integral for time discretization is applied for some nonlinear dispersive wave equations. The Cauchy integral formula plays a vital role in stabilizing the numerical method for this type of nonlinear dispersion equations in the case of nondiagonal large sparse coefficient matrix with extremely small complex eigenvalues. Stability analysis is given by computation in the case of complex linear and nonlinear coefficient. We mainly focus on simulation of the solitary wave of some nonlinear dispersive wave equations. Numerical simulations indicated that the present method is very efficient with loosely restricted CFL condition. As mentioned in Hochbruck and Ostermann (2005), fourth-order convergence cannot be expected, since the stiff order of the scheme might deteriorate down to order 2. However, fourth-order accuracy is still achieved in every test cases in this paper. For further use of present method, the shock wave problem in fluids, such as nonlinear Burgers equations (Yee et al. 2012) or Euler equations (Soni et al. 2017), can also be solved in this way as long as the convection term is treated by efficient shock solvers.

## References

- Apolinar-Fernández A, Ramos JJ (2018) Numerical solution of the generalized, dissipative KdV-RLW-Rosenau equation with a compact method. *Commun. Nonlinear Sci. Numer. Simul* 60:165–183
- Bahadır AR (2005) Exponential finite-difference method applied to Korteweg-de Vries equation for small times. *Appl. Math. Comput.* 160(3):675–682
- Cai J, Liang H, Zhang C (2018) Efficient high-order structure-preserving methods for the generalized Rosenau-type equation with power law nonlinearity. *Commun. Nonlinear Sci. Numer. Simul.* 59:122–131
- Cox SM, Matthews PC (2002) Exponential time differencing for stiff systems. *J. Comput. Phys.* 176(2):430–455
- Cui Y, Mao DK (2007) Numerical method satisfying the first two conservation laws for the Korteweg-de Vries equation. *J. Comput. Phys.* 227(1):376–399
- Du Q, Zhu W (2005) Analysis and applications of the exponential time differencing schemes and their contour integration modifications. *Bit Numer. Math.* 45(2):307–328
- Ghiloufi A, Omrani K (2017) New conservative difference schemes with fourth-order accuracy for some model equation for nonlinear dispersive waves. *Numer. Methods Part. Differ. Equ.* 34(2):451–500
- Gürarslan G (2010) Numerical modelling of linear and nonlinear diffusion equations by compact finite difference method. *Appl. Math. Comput.* 216(8):2472–2478
- Hochbruck M, Ostermann A (2005) Explicit exponential Runge–Kutta methods for semilinear parabolic problems. *SIAM J. Numer. Anal.* 43(3):1069–1090
- Hu J, Wang Y (2013) A high-accuracy linear conservative difference scheme for Rosenau-RLW equation. *Math. Prob. Eng.* 2:841–860
- Kassam A, Trefethen LN (2005) Fourth-order time-stepping for stiff PDEs. *SIAM J. Sci. Comput.* 26(4):1214–1233
- Korteweg DJ, De Vries G (1895) On the change of form of long waves advancing in a rectangular canal, and on a new type of long stationary waves. *Philos. Mag. Ser. 1* 39(240):422–443
- Lele SK (1992) Compact finite difference schemes with spectral-like resolution. *J. Comput. Phys.* 103(1):16–42
- Li J, Y T Chen (2008) *Computational partial differential equations using MATLAB*. CRC Press
- Li J, Visbal MR (2006) High-order compact schemes for nonlinear dispersive waves. *J. Sci. Comput.* 26(1):1–23
- Pan X, Zhang L (2012) On the convergence of a conservative numerical scheme for the usual Rosenau-RLW equation. *Appl. Math. Model.* 36(8):3371–3378
- Park MA (1990) On the Rosenau equation. *Comput. Appl. Math.* 9(2):145–152
- Peregrine DH (1966) Calculations of the development of an undular bore. *J. Fluid Mech.* 25(02):321–330
- Peregrine DH (1967) Long waves on a beach. *J. Fluid Mech.* 27(4):815–827

- Qiu Y, Chen W, Nie Q (2019) A hybrid method for stiff reaction–diffusion equations. *Disc Cont Dyn Syst Ser B* 24(12):6387
- Razborova P, Triki H, Biswas A (2013) Perturbation of dispersive shallow water waves. *Ocean Eng* 63(4):1–7
- Rosenau P (1986) A quasi-continuous description of a nonlinear transmission line. *Physica Scripta* 34:827–829
- Rosenau P (1988) Dynamics of dense discrete systems. *Progress Theor Phys* 79:1028–1042
- Sari M, Gürarşlan G (2009) A sixth-order compact finite difference scheme to the numerical solutions of Burgers equation. *Appl Math Comput* 208(2):475–483
- Soni V, Roussel O, Hadjadj A (2017) On the accuracy and efficiency of point-value multiresolution algorithms for solving scalar wave and Euler equations. *J Comput Appl Math* 323:159–175
- Thacher HC, Henrici P (1974) Wiley, Applied and computational complex analysis
- Trefethen LN (2000) Spectral methods in MATLAB (Software, Environments, Tools). *SIAM* 29(1):209–228
- Wang X, Dai W (2017) A three-level linear implicit conservative scheme for the Rosenau-KdV-RLW equation. *J Comput Appl Math* 330:295–306
- Wang YM, Zhang HB (2009) Higher-order compact finite difference method for systems of reaction–diffusion equations. *J Comput Appl Math* 233(2):502–518
- Wang X, Dai W (2019) A conservative fourth-order stable finite difference scheme for the generalized Rosenau-KdV equation in both 1D and 2D. *J Comput Appl Math*:310–331
- Wongsaijai B, Poochinapan K (2014) A three-level average implicit finite difference scheme to solve equation obtained by coupling the Rosenau-KdV equation and the Rosenau-RLW equation. *Appl Math Comput* 245:289–304
- Wongsaijai B, Mouk tonglang T, Sukantamala N, Poochinapan K (2019) Compact structure-preserving approach to solitary wave in shallow water modeled by the Rosenau-RLW equation. *Appl Math Comput* 340:84–100
- Yee HC, SjöGreen B, Hadjadj A (2012) Comparative study of three high order schemes for LES of temporally evolving mixing layers. *Commun Comput Phys* 12(5):1603–1622
- Zhao J, Corless RM (2006) Compact finite difference method for integro-differential equations. *Appl Math Comput* 177(1):271–288

**Publisher's Note** Springer Nature remains neutral with regard to jurisdictional claims in published maps and institutional affiliations.